Monthly Notices of the ROYAL ASTRONOMICAL SOCIETY

MNRAS **465,** 2160–2169 (2017) doi:10.1093/mnras/stw2838
Advance Access publication 2016 November 3

A JVLA survey of the high-frequency radio emission of the massive magnetic B- and O-type stars

Sushma Kurapati,[1⋆] Poonam Chandra,[1⋆] Gregg Wade,[2⋆] David H. Cohen,[3] Alexandre David-Uraz,[4] Marc Gagne,[5] Jason Grunhut,[6] Mary E. Oksala,[7,8] Veronique Petit,[4] Matt Shultz,[2,9] Jon Sundqvist,[10,11] Richard H. D. Townsend[12] and Asif ud-Doula[13]

[1]*National Centre for Radio Astrophysics, Tata Institute of Fundamental Research, PO Box 3, Pune 411007, India*
[2]*Department of Physics, Royal Military College of Canada, PO Box 17000, Station Forces, Kingston, Ontario K7K 7B4, Canada*
[3]*Department of Physics and Astronomy, Swarthmore College, Swarthmore, PA 19081, USA*
[4]*Department of Physics and Space Sciences, Florida Institute of Technology, Melbourne, FL 32901, USA*
[5]*Department of Earth and Space Sciences, West Chester University, West Chester, PA 19383, USA*
[6]*Dunlap Institute for Astronomy and Astrophysics, University of Toronto, Rm 101, 50 St. George Street, Toronto, ON M5S 3H4, Canada*
[7]*Department of Physics, California Lutheran University, 60 West Olsen Road #3700, Thousand Oaks, CA 91360, USA*
[8]*LESIA, Observatoire de Paris, PSL Research University, CNRS, Sorbonne Universités, UPMC Univ. Paris 06, F-92195 Meudon, France*
[9]*Department of Physics, Engineering Physics and Astronomy, Queen's University, 99 University Avenue, Kingston, ON K7L 3N6, Canada*
[10]*KU Leuven, Instituut voor Sterrenkunde, Celestijnenlaan 200D, B-3001 Leuven, Belgium*
[11]*Centro de Astrobiologia, CSIC-INTA, Departamento de Astrofisica, Ctra. Torrejon a Ajalvir km E-428850 Madrid, Spain*
[12]*Department of Astronomy, 2535 Sterling Hall 475 N. Charter Street, Madison, WI 53706-1582, USA*
[13]*Penn State Worthington Scranton, 120 Ridge View Drive, Dunmore, PA 18512, USA*

Accepted 2016 November 1. Received 2016 November 1; in original form 2016 September 19

ABSTRACT

We conducted a survey of seven magnetic O-type stars and eleven B-type stars with masses above 8 $M_\odot$ using the Very Large Array in the 1, 3 and 13 cm bands. The survey resulted in a detection of two O- and two B-type stars. While the detected O-type stars – HD 37742 and HD 47129 – are in binary systems, the detected B-type stars, HD 156424 and ALS 9522, are not known to be in binaries. All four stars were detected at 3 cm, whereas three were detected at 1 cm and only one star was detected at 13 cm. The detected B-type stars are significantly more radio luminous than the non-detected ones, which is not the case for O-type stars. The non-detections at 13 cm are interpreted as due to thermal free–free absorption. Mass-loss rates were estimated using 3 cm flux densities and were compared with theoretical mass-loss rates, which assume free–free emission. For HD 37742, the two values of the mass-loss rates were in good agreement, possibly suggesting that the radio emission for this star is mainly thermal. For the other three stars, the estimated mass-loss rates from radio observations were much higher than those expected from theory, suggesting either a possible contribution from non-thermal emission from the magnetic star or thermal or non-thermal emission due to interacting winds of the binary system, especially for HD 47129. All the detected stars are predicted to host centrifugal magnetospheres except HD 37742, which is likely to host a dynamical magnetosphere. This suggests that non-thermal radio emission is favoured in stars with centrifugal magnetospheres.

Key words: radiation mechanisms: general – stars: magnetic field – stars: massive – radio continuum: stars.

1 INTRODUCTION

Recent systematic surveys of the magnetic properties of hot stars (MiMeS and BoB surveys; Morel et al. 2014; Wade et al. 2016) have revealed a population of O- and B-type stars hosting significant surface magnetic fields (Petit et al. 2013; Shultz 2016). These magnetic fields are strong (from a few hundred to tens of thousands of gauss), organized (mainly dipolar) and highly stable.

Theoretical models and magnetohydrodynamical (MHD) simulations have explored the dynamical interaction of these magnetic fields with stellar rotation and mass-loss (e.g. ud-Doula &

⋆ E-mail: sushma@ncra.tifr.res.in (SK); poonam@ncra.tifr.res.in (PC); wade-g@rmc.ca (GW)

Owocki 2002; Owocki, Townsend & Ud-Doula 2008). Both observation and theory show clearly that the stellar wind interaction with the magnetic field leads to wind confinement and channelling, generating a long-lived circumstellar magnetosphere (e.g. Shore et al. 1990; Babel & Montmerle 1997). Close to the star, the magnetic pressure dominates the kinetic pressure of the wind, forcing the wind to follow closed magnetic field lines in regions near the magnetic equatorial plane. Far from the star, the kinetic pressure dominates the magnetic pressure due to the stronger decline of the magnetic energy density compared to the wind kinetic energy density. The radius at which the energy densities become equal is defined as the Alfvén radius, which also marks the boundary of the inner magnetosphere. Beyond the Alfvén radius, the stellar wind opens the magnetic field lines and generates a current sheet in the magnetic equatorial plane. This region is the middle magnetosphere, where the electrons are accelerated to relativistic speeds and gyrosynchrotron radio emission is expected to arise (Trigilio et al. 2004). The gyrosynchrotron emitting region extent is defined by these wind electrons returning to the star along the field lines.

Petit et al. (2013) classified the magnetospheres into two broad physical categories, namely dynamical magnetospheres (DMs) and centrifugal magnetospheres (CMs). This classification is based on two parameters: the degree of magnetic wind confinement characterized by the Alfvén radius (R_A), and stellar rotation characterized by the Kepler co-rotation radius (R_K). A DM results in the case of a slowly rotating star ($R_A < R_K$). In this case, wind plasma trapped in closed magnetic loops falls back on to the stellar surface on a dynamical time-scale. A CM occurs in the case of a rapidly rotating star($R_A > R_K$). In this case, wind plasma caught in the region between R_A and R_K is centrifugally supported against infall. This results in long-term accumulation of plasma and consequently higher magnetospheric plasma density.

In stars with high mass-loss rates, radio emission is usually produced by thermal free–free emission from the ionized stellar wind. However, as discussed above, non-thermal synchrotron emission may dominate the radio spectrum in the presence of the magnetic field and relativistic electrons. Electrons can be accelerated to relativistic speeds, either by magnetic reconnection near the current sheet in the middle magnetosphere (Usov & Melrose 1992) or through Fermi acceleration in strong shocks in the inner magnetosphere (Owocki & Rybicki 1984; Eichler & Usov 1993). Thermal radio emission, X-ray emission and optical-line emission are produced from the inner magnetosphere, whereas non-thermal radio emission comes from the middle magnetosphere. Hence, non-thermal radio emission probes different regions of the magnetosphere. In addition, as the emitting plasma is optically thick at long wavelengths, radio radiation at different frequencies probes the stellar magnetosphere at different depths, and from different perspectives as the star rotates. As a consequence, magnetic stars show radio flux variability with the stellar rotation period. The rotation modulation in radio emission was first suggested by Leone (1991) for a rigidly rotating magnetosphere. These modulations have been observed in the radio light curves of some magnetic B–A stars (e.g. Bailey et al. 2012; Chandra et al. 2015) and have been then modelled by Trigilio et al. (2004) and Leto et al. (2006, 2012).

Some numerical simulations (van Loo, Runacres & Blomme 2005) suggest that one requires both a magnetic field and a binary companion to explain the non-thermal radio emission from massive stars. In these simulations, the synchrotron radiation from single massive stars is produced relatively close to the star. Due to the large free–free opacity of the stellar winds at radio wavelengths, radiation emitted too close to the star will be absorbed (Blomme 2011). When a star has a massive nearby binary companion (orbital period of a few days), emission is produced from the wind collision region where shocks occur, which can escape due to a lower free–free opacity (van Loo et al. 2005). Thus, the observed radio flux is likely to have a contribution due to the colliding wind in addition to the star's magnetosphere and thermal free–free emission from the star.

Various investigations have been carried out to observe the radio emission of magnetic A- and B-type stars (e.g. Abbott, Bieging & Churchwell 1985; Drake et al. 1987; Linsky, Drake & Bastian 1992). However, no such studies have been made of the radio properties of hotter magnetic B- and O-type stars. Bieging, Abbott & Churchwell (1989) carried out a Very Large Array (VLA) survey on 88 O-type and early B-type stars, which are not known to be magnetic. They detected a total of 14 sources at 6 cm with six of them displaying non-thermal radio emission. They concluded that non-thermal radio emission is more common in very luminous stars.

To homogenize the study of the physics of magnetospheres of hot stars, we are carrying out a systematic survey of the radio emission properties of the known magnetic O- and B-type stars at high frequencies using the Karl J. Jansky Very Large Array (JVLA) and at low frequencies using the Giant Metrewave Radio Telescope (GMRT). This paper reports the high-frequency JVLA observations. Chandra et al. (2015) reported GMRT observations of the eight magnetic B-type stars and the three magnetic O-type stars. Out of the eight B-type stars, five were detected in both the 1390 and 610 MHz bands. The three O-type stars were observed only in the 1390 MHz band, and no detections were obtained. This result was explained as a consequence of free–free absorption by the freely flowing stellar wind exterior to the confined magnetosphere. The low-frequency GMRT survey thus puts strong constraints on the free–free absorption of radio emission, and combined with high-frequency VLA data can provide a more complete description of the characteristics of the medium surrounding the star.

In this paper, we present results of the JVLA observations of 18 known magnetic O- and B- type stars with masses $M \geq 8\,M_\odot$. In Section 2, we describe the observations and data analysis. In Section 3, we report the detections and the mass-loss rates that are calculated from radio fluxes. In Section 4, we compare the properties of the detected and non-detected stars and explore their properties. In Section 5, we present our conclusions.

2 OBSERVATIONS AND DATA ANALYSIS

2.1 Sample

The basis for target selection is the complete list of known magnetic OB stars compiled by Petit et al. (2013). From this list, we have selected all the stars with mass $\geq 8\,M_\odot$ and declination above -40°. This sample consists of seven O-type stars and eleven B-type stars. The list of targets, along with their stellar parameters from Petit et al. (2013), Nazé et al. (2014) and Shultz (2016), are given in Table 1.

2.2 Observations

The JVLA observations were taken between 2014 March 8 and 2014 August 1 during the 14A semester in the 13 cm (S), 3 cm (X) and 1 cm (Ka) bands. The data were collected in an 8-bit sampler mode for the S band, and in a 3-bit sampler mode for the X and Ka bands. Thus the bandwidths for S, X and Ka bands observations

Table 1. Stellar and magnetic properties (spectral type, distance, luminosity, effective temperature, mass, radius, polar strength of the magnetic field, rotation period, Alfvén radius, Kepler corotation radius and wind terminal velocity) for the sample of magnetic O- and B-type stars.

ID	Name	Binary Comp.	Sp.type	d (pc)	$\log(L_*)$ ($L_\odot$)	$T_{\rm eff}$ (kK)	M_* ($M_\odot$)	R_* ($R_\odot$)	$B_{\rm p}$ (kG)	Period (days)	$R_{\rm A}$ (R_*)	$R_{\rm K}$ (R_*)	v_∞ (km s^{-1})	Binary status
1	HD 191612	Primary	Of?p	2290	5.4 ± 0.2	35 ± 1	30	14	2.5	537.2	3.7	57	2119	BIN
		Secondary	B1	–	–	20	15	–	–	–	–	–	–	–
2	NGC 1624-2	–	Of?cp	5152	5.1 ± 0.2	35 ± 2	34	9.7	>20	158	>11	41	2890	–
3	CPD -282561	–	Of?p	6100	5.5 ± 0.2	35 ± 2	43	14	>1.7	73.4	3.4	18.7	2400	–
4	HD 47129	Secondary	O7.5 III	1584	5.31 ± 0.03	37 ± 2	22	11	>2.8	1.21551	>5.4	<2.2	3567	BIN
		Primary	O8 III/I	–	5.14 ± 0.04	32 ± 2	3	12	–	–	–	–	–	–
5	HD 108	–	Of?p	2510	5.7 ± 0.1	35 ± 2	43	19	>0.50	18000	>1.7	526	2022	–
6	HD 57682	–	O9 V	1300	4.8 ± 0.2	34 ± 1	17	7	1.7	63.571	3.7	24	2395	–
7	HD 37742	Primary	O9.5 Ib	414	5.6 ± 0.1	29.5 ± 1	33	20	0.140	7	1.1	2.1	1723	BIN
		Secondary	B1 IV	–	4.4	29	14	7	–	–	–	–	–	–
8	HD 149438	–	B0.2 V	180	4.5 ± 0.1	32 ± 1	17.2	6.0	0.2	41.033	2.0	20.3	2581	–
9	HD 66665	–	B0.5 V	1500	4.2 ± 0.5	28 ± 1	9	5.5	0.67	21	3.1	12.3	2256	–
10	HD 46328	–	B1 III	423	4.6 ± 0.1	27 ± 2	13.4	7.5	>1.5	8600	5.7	867.4	1984	–
11	ALS 8988	–	B1	1880	4.1 ± 0.1	27 ± 1	12	4.7	>1.5	–	>7.5	<9.6	–	–
12	HD 47777	–	B1 III	760	4.1 ± 0.1	27 ± 2	9	5	>2.1	537.2	>8.6	<4.3	2142	–
13	HD 205021	Primary	B1 IV	182	4.2 ± 0.1	26 ± 1	12	6.5	0.36	12.001	3.1	7.3	2064	BIN
	–	Secondary	B5 Ve	–	–	17	4	–	–	–	–	–	–	–
14	HD 163472	–	B1/2 V	290	3.8 ± 0.1	25 ± 1	10.2	4.6	0.40	3.639	7.3	4.5	2344	–
15	ALS 9522	–	B1.5 V	1800	4.0 ± 0.1	22 ± 2	10	6.4	>4.0	–	>11	<2	989	–
16	HD 156424	–	B2 V	1100	3.7 ± 0.4	22 ± 3	7.4	5.0	>0.65	2.87	15.7	3.1	957	–
17	HD 3360	–	B2 IV	183	3.7 ± 0.2	20.4 ± 0.9	8.2	5.7	>0.34	5.371	2.5	4.2	932	–
18	HD 58260	–	B3 Vp	826	4.1 ± 0.2	20 ± 2	8.8	9.5	>7.0	–	14.4	9.9	766	–

Notes. Taken from Petit et al. (2013), Nazé et al. (2014), Hummel et al. (2013), Wheelwright, Oudmaijer & Schnerr (2009) and Shultz (2016) and references therein.

were 2 GHz (frequency range 2–4 GHz), 4 GHz (frequency range 8–12 GHz) and 8 GHz (frequency range 29–37 GHz), respectively. The observations were taken in VLA A, D and A→D configurations. The duration of each observation, including overheads, in S and X bands was 30 min and 1 h for the Ka band. For each observation, a flux calibrator and a phase calibrator were observed along with the target source. The flux calibrator was observed once, either at the start or at the end of the observation. The phase calibrator was observed once every five minutes for the S and X bands and once every three minutes for the Ka-band observations. Approximately 15 min was spent on the target source for S- and X-band observations and 30 min was spent on the target source for Ka-band observations.

2.3 Data analysis

All the calibration and data reduction were carried out using standard tasks in the COMMON ASTRONOMY SOFTWARE APPLICATIONS (CASA) package. The initial reduction steps such as flagging bad data, correcting for atmospheric opacities, antenna delay solutions and bandpass corrections were done using the VLA calibration pipeline. In some cases, additional flagging and recalibration were required after the pipeline calibration. In such cases, flagging was done manually and the pipeline was used again to recalibrate the data. The flagged and calibrated visibility data were used to produce continuum images using the CLEAN algorithm in CASA. Wide-band effects were taken into account using multifrequency synthesis, where two Taylor coefficients were used to model the sky frequency dependence. All the detected sources were unresolved at JVLA frequencies. Flux densities on these radio sources were measured by fitting elliptical Gaussian functions to them using the CASA task IMFIT. Both the uncertainties in the Gaussian fit and the local rms noise were taken into account for calculating the uncertainty in measured flux density. The rms noise, flux densities for the detected sources and 3σ upper limits for the non-detections are included in Table 2.

3 RESULTS

This survey resulted in a total of four detections in the X band. The detected stars are HD 37742 (O9.5 Ib), HD 47129 (O7.5 III), HD 156424 (B2 V) and ALS 9522 (B1.5 V). Three of the stars detected in the X band are also detected in the Ka band (i.e. all except for ALS 9522). Only one of them, HD 37742, was also detected in the S band. The non-detections in the S band are probably due to free–free absorption. This is because, due to the wavelength-squared dependence of the free–free opacity (e.g. Weiler et al. 2002), the size of the radio photosphere increases with wavelength resulting in high free–free absorption at S-band frequencies compared to the X and Ka bands.

3.1 Mass-loss rates

In this section, we estimate the mass-loss rates from our radio observations, and compare them with the mass-loss rates calculated from theoretical models which are based on free–free emission. This may allow us to understand the emission processes and estimate the thermal versus non-thermal contributions to the radio emission. If the radio radiation is purely thermal, we would expect that the mass-loss rates estimated from observations to match those expected from the theoretical models. If the radio emission has an important non-thermal contribution, then our estimates based on the thermal emission assumption are likely to be overestimates.

The theoretical mass-loss rates were taken from Nazé et al. (2014). They used the models of Vink, de Koter & Lamers (2000) as a function of effective temperature, mass, luminosity and wind

Table 2. VLA Observations of magnetic O- and B-type stars.

Name	13 cm				3 cm				1 cm			
	Obs. Date	Flux density (mJy)	rms (μJy)	Mean Phase	Obs. Date	Flux density (mJy)	rms (μJy)	Mean Phase	Obs. Date	Flux density (mJy)	rms (μJy)	Mean Phase
HD 191612	Apr 25.74	<0.037	12	0.17	Apr 23.47	<0.019	6.5	0.24	May 02.60	<0.031	10.3	0.26
NGC 1624-2	May 05.95	<0.024	8	0.17	Apr 29.90	<0.018	6.2	0.13	Aug 01.63	<0.042	14	0.72
CPD -282561	May 05.97	<0.028	9.5	0.12	Apr 29.11	<0.021	7	0.12	–	–	–	–
HD 47129	May 10.91	<0.03	10	0.71	May 06.97	0.208 ± 0.015	7.2	0.47	Jul 13.64	0.392 ± 0.037	13.0	0.13
HD 108	–	–	–	–	May 03.92	<0.019	6.3	–	Jul 12.62	<0.038	12.6	–
HD 57682	Apr 04.87	<0.024	8.2	0.54	Apr 03.95	<0.029	9.8	0.54	Apr 05.21	<0.030	10	0.56
HD 37742	Apr 17.01	0.494 ± 0.025	8.3	0.64	Apr 16.03	1.104 ± 0.015	6	0.50	Jul 29.57	2.765 ± 0.049	15.0	0.43
HD 149438	Apr 29.3	<36	12	–	Apr 25.29	<0.020	6.5	–	May 11.28	<0.035	11.7	–
HD 66665	Apr 30.17	<42	14	0.35	Apr 29.20	<0.018	6	0.31	May 09.16	<0.033	11.0	0.72
HD 46328	Apr 03.99	<45	15	0.14	Apr 03.97	<0.018	6	0.14	Jul 19.64	<0.048	16.0	0.16
ALS 8988	May 12.98	<30	10	–	Apr 29.92	<0.020	6.7	–	Jul 11.67	<0.044	14.8	–
HD 47777	–	–	–	–	Apr 07.90	<0.036	12	–	Apr 08.22	<0.034	11.4	–
HD 205021	Apr 24.59	<0.029	9.8	0.13	Apr 22.60	<0.033	11	0.97	Apr 22.56	<0.034	11.4	0.96
HD 163472	May 05.27	<0.033	11	0.47	Apr 28.29	<0.019	6.3	0.56	Jun 17.18	<0.033	11.2	0.27
ALS 9522	May 23.32	<0.027	9	–	Apr 26.35	0.080 ± 0.012	6		May 13.31	<0.030	10.0	–
HD 156424	–	–	–	–	May 12.31	0.381 ± 0.015	6	0.06	Jun 26.21	0.494 ± 0.028	14.0	0.70
HD 3360	Mar 08.93	<0.029	9.6	0.02	Mar 28.01	<0.018	6	0.57	Jul 11.63	<0.038	12.6	0.24
HD 58260	Apr 25.92	<0.036	12	–	Apr 22.98	<0.042	14	–	Jul 20.71	<0.075	25	–

Notes. the upper limits on the flux densities are 3σ upper limits. All the observations were taken in the year 2014.

Table 3. Theoretical and empirical mass-loss rates of the stars.

Name	$\dot{M}_{\rm th}$ ($\times 10^{-6} M_\odot$ yr^{-1})	$\dot{M}_{\rm obs}$ ($\times 10^{-6} M_\odot$ yr^{-1})
HD 191612	0.79	<0.85
NGC 1624-2	0.16	<3.71
HD 47129	0.06	4.89
HD 108	2.51	<0.93
HD 37742	1.12	1.25
HD 57682	0.08	<0.56
HD 149438	0.02	<0.02
HD 66665	0.006	<0.47
HD 46328	0.03	<0.06
HD 47777	0.002	<0.27
HD 205021	0.002	<0.03
HD 163472	0.0003	<0.04
ALS 9522	0.01	0.67
HD 156424	0.003	1.34
HD 3360	0.004	<0.008

Notes. $\dot{M}_{th}$ is the theoretical mass-loss rate (Vink et al. 2000).

terminal velocity. The model assumes that the star is isolated, neglecting any effects of binarity. They assume that the atmosphere consists of H, He, C, N, O and Si. The model takes multiple scattering into account. The theoretical mass-loss rates correspond to those that the stars would have in the absence of a surface magnetic field. It treats the gas in non-LTE (local thermodynamical equilibrium) with the transfer of radiation computed in an expanding atmosphere. The temperature structure is from the assumption of radiative equilibrium in a spherically symmetric LTE atmosphere. The surrounding medium is also considered to be smooth. Thus, the realistic situation may be far from this ideal, resulting in some uncertainties in theoretical mass-loss rates. However, these uncertainties are likely to change the mass-loss rate by about a factor of 3 (Krtička 2014; Smith 2014), much less than the discrepancies we report in Table 3.

We calculated the expected mass-loss rates from our X-band radio data, assuming the observed radio emission is purely thermal. The free–free radio flux density S_ν in Jy is related to the stellar mass-loss rate $\dot{M}$ by (Bieging et al. 1989):

$$\dot{M} = \frac{3.01 \times 10^{-6} \mu}{Z(\gamma g_{\rm ff} \nu)^{1/2}} V_\infty S_\nu^{3/4} D^{3/2} {\rm M}_\odot {\rm yr}^{-1}, \quad (1)$$

where μ is the mean ionic weight in amu, v_∞ is the terminal velocity in km s^{-1}, D is the distance to the star in kpc, ν is the frequency in GHz, γ is the mean number of electrons per ion, Z is the rms charge per ion and $g_{\rm ff}$ is the free–free Gaunt factor, given by:

$$g_{\rm ff} = -1.66 + 1.27 \log(T_{\rm wind}^{3/2}/(Z\nu)), \quad (2)$$

where $T_{\rm wind}$ is the local temperature (in K) at the radio photosphere.

Table 3 shows the mass-loss rates derived using the above procedure. We also list their respective theoretical mass-loss rates. We have listed only 15 of 18 stars, as only these stars have theoretical mass-loss rates reported in the literature (Nazé et al. 2014). In the case of the stars that are in binary systems, the wind from both the stellar components have not been considered for evaluating theoretical mass-loss rates, which could create some discrepancy in the correct estimation of the mass-loss rate. In three of the detected stars, we find that for HD4 7129, HD 156424 and ALS 9522, the mass-loss rates derived from radio observations are many times higher than those expected from the theoretical models. This could suggest a significant contribution of radio emission by various mechanisms, e.g. non-thermal radio emission or radio emission from a colliding wind binary. For HD 37742, the mass-loss rate obtained from radio observations matches the value obtained using the theoretical model. This result could be evidence for a thermal origin of its radio emission. For the non-detected stars, upper limits on estimated mass-loss rates (from 3σ upper limits on the radio flux) are consistent with the theoretical mass-loss rates for those stars, i.e. the theoretical model predicts radio fluxes that are below our detection threshold.

3.2 Detections

Here we discuss the properties of the detected stars and the nature of their radio emission.

3.2.1 HD 47129

HD 47129 (Plaskett's star; Plaskett 1922) is a massive binary system composed of O8 III/I and O7.5 III stars with an orbital period of 14 d (Linder et al. 2008). A strong, organized magnetic field was detected in the rapidly rotating secondary component (with a dipole polar strength of ∼2800 G; Grunhut et al. 2013), while the primary is not known to host a magnetic field. Grunhut et al. (2013) show that the magnetic star has evidence of magnetic field inversion. This stellar system has been shown to be chemically peculiar, and is a hard, luminous and variable source of X-rays (Linder et al. 2008). The combination of strong magnetic field and rapid rotation leads to the existence of a CM (cf. Petit et al. 2013) surrounding the secondary star (Grunhut et al. 2013). This is in contrast to all other known magnetic O-type stars that host DMs. HD 47129 is proposed to be a post-mass transfer (post-Roche lobe overflow) system, which could explain the observed mass–luminosity mismatch, chemical peculiarity and rapid rotation of the secondary star (Bagnuolo & Gies 1992; Linder et al. 2008).

To phase the observations of Plaskett's star, we used the rotational ephemeris for the magnetic secondary star reported by Grunhut et al. (in preparation):

$$HJD = 2455961.000 + 1.21551 \cdot E. \quad (3)$$

However, there may be evidence for a period change (Grunhut et al., in preparation). The rotation period of this star was determined using a combination of magnetic, spectroscopic and photometric measurements. Grunhut et al. (in preparation) obtained 63 magnetic observations of the system, which they combined with equivalent width measurements of the He II ($\lambda = 4686\text{A}^0$) and Hβ lines and CoRoT photometry, to infer the rotation period of the magnetic component, $P = 1.21551$ d. This period is firmly established, and phase zero corresponds to the phase of maximum longitudinal magnetic field. Radio emission is clearly detected in the X and Ka bands at phases 0.47 and 0.13, respectively, according to equation (3). We cannot unambiguously determine the spectral index of the source using the observations obtained in the various frequency bands as they correspond to different phases. However, due to the larger bandwidth of each band, we attempted to obtain the intraband spectral index. For this purpose, we calculated continuum images using the first half and second half of the band, and flux densities were determined. The spectral index is calculated to be -1.2 ± 1.0 between sub-bands of the X band, i.e. between central frequencies of 9 and 11 GHz. The value of the spectral index in the sub-bands of the Ka band, i.e. between central frequencies of 31 and 35 GHz, is 0.0 ± 2.5. The observed mass-loss rate in this case is roughly two orders of magnitude larger than the theoretical mass-loss rate. This indicates that the radio emission may come from different mechanisms. This star is in a close binary system (orbital period ∼14 d). This radio emission can be due to thermal free–free emission from the ionized medium surrounding the individual components of the binary and non-thermal radio emission from CM surrounding the magnetic secondary star. In addition, in this close binary system, interacting winds of the binary system can also give rise to the thermal as well as the non-thermal radio emission.

3.2.2 HD3 7742

HD 37742 (ζ Orionis A) is the closest O star in our sample. It is an O-type binary star and is one of the belt stars in the constellation Orion. It was shown to be a binary system composed of a O9.5I supergiant and a B1IV star with an orbital period of 2687 d (Hummel et al. 2013). Bouret et al. (2008) determined the primary component ζ Ori Aa to be a 40 $M_\odot$ star with a radius of 25 $R_\odot$ at an age of 5 to 6 Myr, showing no surface nitrogen enhancement and losing mass at a rate of about $2 \times 10^{-6}\,M_\odot yr^{-1}$. The magnetic field of the primary star is the weakest magnetic field ever detected on a massive star (∼140 G; Blazère et al. 2015). Magnetic field is not detected on its companion ζ Ori Ab with an upper limit of ∼300 G. Because the magnetic field and the rotation rate are weak and the stellar wind is strong, ζ Ori Aa does not host a CM. However, it may host a weak DM. Although this star is also well known for its prominent X-ray emission, Cohen et al. (2014) found that the emission resembles that of a non-magnetic star in the X-ray domain. This is consistent with the negligible magnetospheres surrounding ζ Ori Aa.

To phase the observations, we have used the rotational ephemeris given by Bouret et al. (2008):

$$HJD = 2454380.0 + 6.829 \cdot E. \quad (4)$$

HD 37742 is detected in the S, X and Ka bands. The star has higher flux density in the Ka band as compared to the S and X bands. The intra-band spectral index was found to be 0.3 ± 0.3 in the S-band, 0.5 ± 0.2 in the X-band and 0.7 ± 0.4 in the Ka band. The positive spectral index in all bands suggest that the emission has a significant contribution from thermal emission. This star was previously observed by Lamers & Leitherer (1993) at 3.6 and 6 cm. The reported flux densities are 0.89 ± 0.04 mJy at 3.6 cm and 0.7 mJy at 6 cm. They concluded that the emission from this star is thermal using the slope for the spectrum and the absence of polarization. Comparison with the observed Hα emission also suggested that the star does not exhibit significant non-thermal emission at centimetre wavelengths (Lamers & Leitherer 1993). In addition, this is the only detected star for which the values of the observational and theoretical mass-loss rates are consistent with each other, again suggesting a thermal origin of the radio emission. This may indicate that its magnetosphere – expected to be very small – is not contributing significantly to the radio emission from this star. Though, this star is in a binary system, longer orbital period (∼2687 d) suggests that winds of the individual stars may not be interacting. So, the radio emission is not likely to come from the wind colliding region.

Since thermal emission is likely to be independent of the rotational phase of the star, we can plot the flux densities at various frequencies irrespective of their phases. Fig. 1 shows the flux density versus frequency in the S, X and Ka bands. We have also included the flux densities at 5 and 8.3 GHz from Lamers & Leitherer (1993). The spectral index is found to be 0.76 ± 0.03, suggesting that the emission is thermal. The spectral index can be used to infer information about the steepness of the density gradient. A spectral index of ∼0.6 is expected in the case of a stellar envelope in which the electron density (n_e) is proportional to r^{-2}, starting from the photospheric radius up to infinity (Olnon 1975; Panagia & Felli 1975). Assuming a smooth density profile, we can obtain the density structure around the star, which is found to be $n_e \propto r^{-2.2}$. However, a clumpy medium can also change the value of the spectral index.

3.2.3 ALS 9522

ALS 9522 (W601) is a B1.5V star and a member of the open cluster NGC 6611 (Dufton et al. 2006). This star has been classified as a pre-main-sequence star and is an evolutionary progenitor of a main-sequence B star (Martayan et al. 2007). A magnetic field was detected in this star by Alecian et al. (2008), implying a dipole

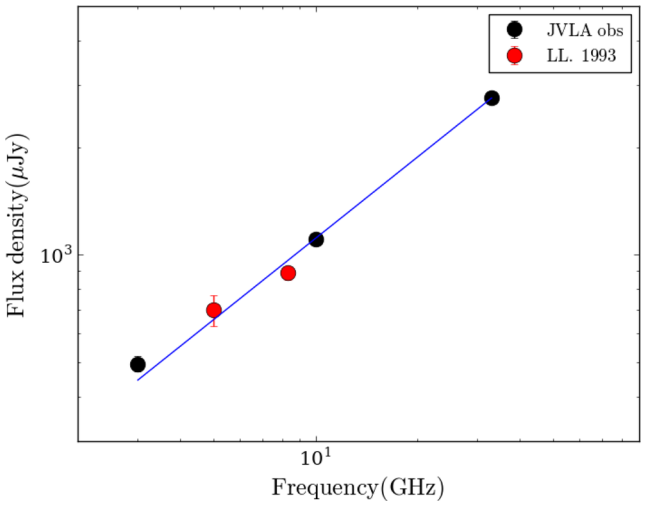

Figure 1. Log–log plot of flux density versus frequency for HD 37742. Flux densities at 5 and 8 GHz were taken from Lamers & Leitherer (1993). Blue line is a power-law fit to the observations with a spectral index of ∼0.7, indicating thermal emission. The JVLA data points have error bars but the error bars are smaller than the symbol size. The 8 GHz data from Lamers & Leitherer (1993) does not have error bars.

field of roughly 4 kG (Petit et al. 2013). The existence of such a magnetic field in a pre-main-sequence star supports the fossil field hypothesis, which supposes that the magnetic field is a relic from the field present in the interstellar medium from which the star was formed. The star is also known to be an X-ray emitter (Guarcello et al. 2012). This star was detected in the X-band, but was not detected in the S and Ka bands. No ephemeris for this star is available, hence we could not calculate the phases corresponding to the different observations.

However, the longitudinal magnetic field observations of Alecian et al. (2008) show strong variability, suggesting that rotational modulation will be significant.

Out of the detected stars at X-band, this is the only star which is not detected at the Ka band, which may be indicative of non-thermal emission. This is supported by the fact that the observational estimate of the mass-loss rate is roughly two orders of magnitude larger than the theoretical rate.

3.2.4 HD 156424

HD 156424 is an He-strong B2V star belonging to the Sco OB4 association (Kharchenko et al. 2004). A magnetic field was detected by Alecian et al. (2014) in the MiMeS survey, Further monitoring by Shultz (2016) identified the system as a radial velocity variable and candidate SB1 star, and allowed the derivation of a dipole magnetic field strength of 5.4 kG. Of the four targets detected in the radio, this is the only star that has not been detected in the X-rays (Nazé et al. 2014). They derived an upper limit on the $0.5 - 10$ keV X-ray flux of $\log(L_X) < 29.8$ erg s^{-1}. ud-Doula et al. (2014) carried out 2D MHD simulations to examine the effects of radiative cooling and inverse Compton cooling on X-ray emission in magnetic massive stars with radiatively driven stellar winds. In their semi-analytic scaling analysis, they estimated the X-ray flux for this star to be $\log(L_X) = 29.7$ erg $^{-1}$, which is compatible with the observational upper limits.

We have used the ephemeris of Shultz (2016) to phase our observations:

$$HJD = 2456126.664 + 2.87233 \cdot E. \quad (5)$$

The rotation period of this star was determined using a combination of magnetic, spectroscopic and photometric measurements. Shultz et al. (in preparation) obtained 11 magnetic measurements of HD 156424 which they combined with a dozen high-resolution spectra. Both magnetic and Halpha EW measurements combine to suggest period of 2.8721 d. The zero-point corresponds to the largest unsigned longitudinal field. This star is detected in the X and Ka bands, but it was not observed in the S-band. The flux density at 33 GHz is higher than the flux density at 10 GHz. However, this could reflect the slope of the spectral energy distribution, or it might be due to flux variability between different phases. In order to obtain an estimate of the spectral index, we have evaluated the flux densities using the first half and second half of the X and Ka bands. Evaluated intra-band spectral indices are -0.5 ± 0.5 and -1.3 ± 2.0 at the X and Ka bands, respectively. The observational estimate of the mass-loss rate for this star is nearly 500 times the theoretical rate, strongly implying an important non-thermal contribution to its emission.

4 DISCUSSION

In this section, we examine relationships between the measured radio properties of the detected and non-detected magnetic stars and their magnetospheric properties.

Fig. 2 shows the location of the observed stars in a log–log plot of R_A/R_K versus the effective temperature (upper frame) and the radio luminosity at 10 GHz (lower frame). The horizontal line in both the plots at $R_A = R_K$ shows the theoretical division between stars hosting CMs (upper region) and DMs (lower region). The distance of a target above the horizontal line characterizes the radial extent of the centrifugal support, and serves as a proxy for the volume of the CM. We note that all of the detected stars host CMs except for HD 37742, which likely hosts a DM (Blazère et al. 2015). Comparison of mass-loss rates (Section 3.1) and spectral index (Section 3.2) suggests that the emission from HD 37742 is thermal. It appears that non-thermal radio emission seems to favour CMs. This is qualitatively expected, as electrons can be more easily accelerated to relativistic speeds in the high-density plasma of a CM to produce non-thermal emission (Trigilio et al. 2004).

Radio luminosities plotted in Fig. 2 are calculated from the radio flux densities in the X band. Upper limits on radio luminosities were calculated from 3σ upper limits on flux densities for the non-detections. We attempted to determine if the radio luminosity depends upon the stellar properties such as effective temperature or magnetic field. Fig. 3 shows the log–log plot of radio luminosity versus the effective temperature (upper frame) and the dipole magnetic field (lower frame). Radio luminosities show no correlation with effective temperature, nor do they show any relationship with magnetic field strength. Among the radio-detected stars, HD 37742 has very weak magnetic field. The remaining detected stars have magnetic fields of similar strength to those of the population of undetected stars.

We can compare the radio detections of our sample of magnetic stars to the VLA survey of 88 non-magnetic OB stars carried out by Bieging et al. (1989). Those authors detected a total of 14 sources at 6 cm. They observed non-thermal emission in six of the stars and free–free emission in eight stars. The criterion used for establishing the nature of radio emission is the radio spectrum. They looked at

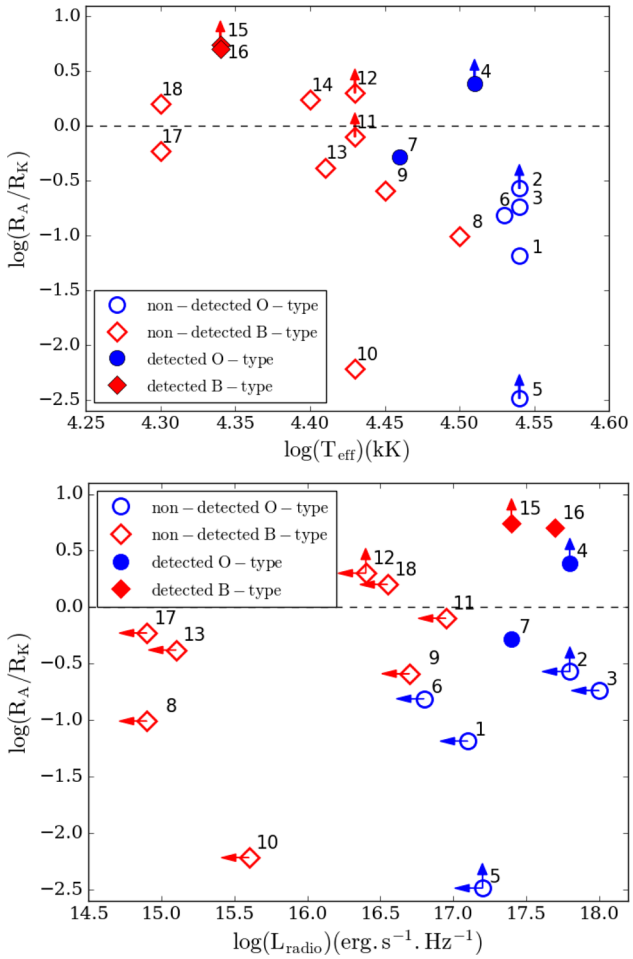

Figure 2. Location of magnetic B- and O-type stars in a log–log plot of R_A/R_K versus effective temperature (top panel) and radio luminosity (bottom panel). The horizontal line in both plots shows the division between centrifugal magnetospheres (area above the line) and dynamical magnetospheres (area below the line). Blue circles indicate the O-type stars and red diamonds indicate the B-type stars. Filled symbols indicate the radio-detected stars. The labels refer to ID sequence number listed in Column 1 of Table 1.

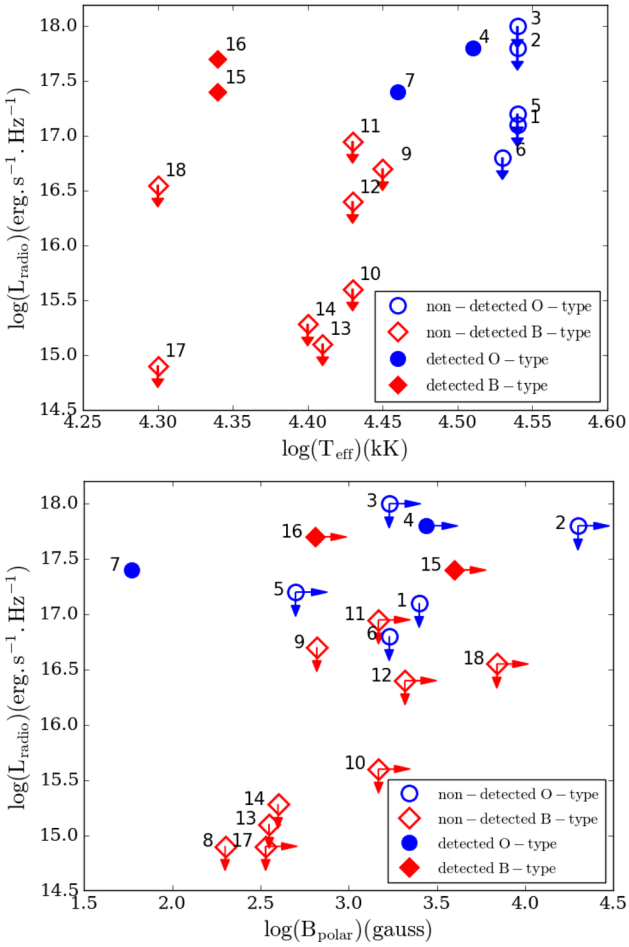

Figure 3. Location of magnetic O- and B-type stars in a log–log plot of radio luminosity versus effective temperature (top) and dipole magnetic field strength (bottom). Blue circles indicate O-type stars and red diamonds indicate B-type stars. Filled symbols indicate radio detections. Upper limits on luminosities were calculated from 3σ upper limits on flux densities. The labels refer to the ID sequence number listed in Column 1 of Table 1.

the general shape of spectrum at different epochs, and found that the non-thermal emission was more efficient in optically luminous stars. However, we did not find any correlation of detections with their optical luminosities.

Nazé et al. (2014) studied the X-ray emission of the magnetic OB stars, which contains all the stars in our sample. They found that the two O stars (HD 37742 and HD 47129) show distinct X-ray properties, indicating that the main origin of the X-ray emission is most probably non-magnetic. Both of these O stars are detected in radio bands.

We discuss the results and properties of the O- and B-type stars from our sample in the following subsections in detail.

4.1 O-type stars

Two out of seven O-type stars were detected in our VLA observations. All the O-type stars have DMs except for radio detected Plaskett's star (HD 47129). This is not surprising, as all the O-type stars have strong stellar winds due to their high luminosities, which implies a rapid stellar spin-down due to magnetic braking. As Plaskett's star is in a close binary system, it was probably spun up due to binary interaction (e.g. Grunhut et al. 2013).

The other radio detected star HD 37742 may host a weak magnetic field, and may not have much contribution from the magnetosphere. This has been confirmed as the comparison of mass-loss rates (Section 3.1) and spectral index (Section 3.2) strongly suggest that the emission from HD 37742 is thermal.

On the contrary, the mass-loss rate of HD 47129 is two orders of magnitude larger than the theoretical estimate. This is a close binary system consisting of the O-type stars, with the secondary having a well ordered large scale magnetic field. In addition to thermal free–free emission from the ionized medium surrounding the individual components of the binary, a CM surrounding the magnetic secondary star could be a source of non-thermal radio emission. In addition, in this close binary system, interacting winds of the binary can also give rise to thermal as well as non-thermal radio emission (Stevens 1995; Pittard 2010). Thus the total radio emission in a close binary will be due to thermal components from individual stars, as well as thermal and non-thermal component from

the colliding wind region (Pittard 2010). Stevens (1995) investigated the total thermal flux from colliding wind binaries and found that it could be about 50 per cent higher than that expected from the free-streaming stellar wind alone. MHD simulations by Pittard (2010) have shown that the thermal component due to the colliding wind will start to dominate at high frequencies ∼50 GHz, whereas the non-thermal component coming from the magnetosphere is likely to be absorbed. At lower frequencies, emission from individual stars will be important.

However, if the stars in the binary system have large separation, the wind interaction is not likely to be effective. For example, HD 37742 is in a binary system, but with a much longer orbital period (∼2687 d) and radio emission is explained well by the free–free emission of the ionized wind of the star, without any need to incorporate wind interaction.

Binarity remains a fundamental question regarding the non-thermal radio emission from the O-type stars. van Loo et al. (2005) concluded that non-thermal radio emission from the O stars cannot be explained by wind-embedded shocks, and is likely to be caused by a colliding wind shock. That would imply that all the O stars with non-thermal radio emission should be members of binary or multiple system. Of the 16 currently known non-thermal radio emitting stars, 15 are confirmed binaries (van Loo, Runacres & Blomme 2006), however none of them is known to be a magnetic star. In our sample, two of the detected O-type stars are known to be binaries. However, only HD 47129 could be in the limit of being classified as colliding wind binary, with an orbital period of ∼14 d. Other binary stars have much longer orbital periods, indicating large binary separations. Simultaneous observations of HD 47129 at different frequencies are required to understand if the emission is thermal or non-thermal, and to investigate any relationship with the binary properties of the system. Observations on a larger sample of O-type stars may shed more light on correlation of binarity with non-thermal radio emission.

The spectral index measurements may also be able to throw light on radio emission mechanism. We estimate a spectral index α ranging from -0.2 to -2.2, between 9 and 11 GHz frequencies. If the radio emission from HD 47129 is purely non-thermal, the lowest expected flux density at 3 GHz is about 0.26 mJy using $\alpha = -0.2$. Linsky et al. (1992) estimated the minimum flux density to be about 50 per cent of the maximum [typically for magnetic chemically peculiar (MCP) stars] for oblique rotators, if the radio emission is modulated. Thus one should have expected a flux density of ∼0.13 mJy at 10 cm, easily detectable at JVLA sensitivity. Thus the non-detection of HD 47129 at 10 cm suggests that a significant contribution may come from the wind–wind interaction in this close binary system.

We have searched the literature for single O-type stars that are thermal radio sources from the literature. While their numbers are handful, their theoretical mass-loss rates are in good agreement with mass-loss rates derived from their radio fluxes (Bieging et al. 1989; Lamers & Leitherer 1993; Benaglia, Cappa & Koribalski 2001). The radio luminosities of the detected O-type stars are similar to the upper limits of the non-detected O-type stars. Hence it is not clear whether the detected O-type stars exhibit radio luminosities that are quite different from those of the overall population of the magnetic O stars (i.e. the high-luminosity tail of a broad distribution), or if they represent only marginally brighter examples of a more uniform distribution. One surprising result is the lack of any detection of radio emission from NGC 1624-2, the star with the strongest magnetic field of the sample (by nearly an order of magnitude). The observations of this star yield a 3σ upper limit that is similar to that of the other non-detected O-type stars. Strong absorption by wind created from mass-loss could explain this.

4.2 B-type stars

Both the detected B-type stars, HD 156424 and ALS 9522, host a CM and lie above all the non-detected B-type stars in Fig. 2. This implies that both the detected stars have a larger radial extent of centrifugal support of magnetospheric plasma compared to the non-detected stars.

The detected B-type stars are significantly more radio luminous than the majority of the upper limits of the non-detected B-type stars. In fact, for all but three of the undetected B-type stars, the radio luminosity upper limits are at least an order of magnitude below the detected stars. This implies that the radio emission properties of the detected stars are, statistically speaking, very different from those of the undetected stars.

In the case of the detected B-stars, the implied mass-loss rates are much higher than the theoretical estimates. Since the detected B stars are not known to be in binaries, the excess flux is likely to be a contribution from the magnetosphere from the magnetic star.

We can compare the radio detections of the B-type stars in our sample to the VLA survey of MCP stars carried out by (Linsky et al. 1992). They have detected a total of 16 out of 61 sources at 6 cm. They found a wide range of 6 cm radio luminosities for the detected Bp stars, with $\log(L_{6\,\mathrm{cm}}) = 15.7$–$17.9$. The detected B-type stars from our sample have radio luminosities of 17.4 and 17.7 at 3 cm. These values lie within the broad range of MCP stars. They have also found that the radio luminosities of MCP stars correlate positively with effective temperature and magnetic field strength. However, no such correlations were found for the B-type stars in our sample.

5 SUMMARY AND CONCLUSIONS

We have initiated a systematic survey of the radio emission properties of the known magnetic OB stars, which includes observations at both high frequencies using the JVLA and at low frequencies using the GMRT. The project is ongoing. In this paper, we have presented the results of JVLA observations of 18 magnetic O- and B-type stars with masses greater than $8\,M_{\odot}$. The JVLA observations were taken at random rotational phases in the S, X and Ka bands. We have detected X-band radio emission from two out of seven magnetic O-type stars and 2 out of 11 magnetic B-type stars in our sample. The detected O-type stars, HD 37742 and HD 47129, are in binary systems.

The detected B-type stars, HD 156424 and ALS 9522, are not known to be in binaries. Two other O-type stars, which are known to be in (much longer-period) binary systems (HD 108, HD,191612) were not detected. Only HD,37742 is detected in the S band. The general lack of detections of our targets in the S-band is probably due to free–free absorption by the free-streaming stellar wind. Three stars, HD,37742, HD 47129 and HD 156424, were detected in the Ka band. The radio flux of HD 37742 and HD 47129 in the Ka band is consistently higher compared with that in the S and X bands. This can be explained by a dominant contribution of thermal flux.

Mass-loss rates were estimated for the detected stars using the X-band radio flux densities and were compared with the expected

mass-loss rates from the theoretical models. However, there are some caveats in theoretical prediction of mass-loss rates as binarity and the presence of magnetic field were not taken into account. In addition, the theoretical estimates assume smooth density profiles, while clumping factors of order 10 are measured in the O-type star winds. However, the clumpiness of the medium is not expected to change the mass-loss rate by more than a factor of 3 (Smith 2014), much less than the discrepancy we note. For HD 37742, the theoretical estimate matches with that of the observational one, suggesting that the radio emission is mostly thermal. The thermal nature of the HD 37742 radio emission is also supported by the spectral index we measure. For the remaining three stars, mass-loss rates estimated from radio observations were orders of magnitude higher compared to those predicted by theory. This may indicate significant contribution of the radio emission from other mechanisms than only thermal free–free emission. In magnetic stars, middle magnetosphere can give rise to non-thermal gyrosynchrotron emission. However, in case of binary systems, the stellar wind from both the stars may interact and produce thermal and non-thermal emission. The detected B- stars in our sample are not known to be in binary system, thus the additional mass-loss rate is likely to have contribution from the non-thermal emission of the magnetosphere. However, HD 47129 is a close binary system and emission from colliding stellar winds could play a significant role.

All the detected stars host CMs except for HD 37742, which hosts a DM. However, the radio emission of HD 37742 is unambiguously thermal. This suggests that non-thermal radio emission seems to favour CMs. In addition, binary wind interactions may also play a role.

We were unable to evaluate the nature of emission or variability of radio flux as we have adopted a snapshot approach to identify the stars that are emitting radio radiation. In order to understand the emission mechanisms and flux variability over the rotation period, we need to observe the detected stars simultaneously over all the frequencies.

The detectability of the O-type stars seems to be sensitivity limited. With the upcoming Square Kilometre Array, we expect to achieve a significant sensitivity and detect a larger fraction of the O star sample.

ACKNOWLEDGEMENTS

We thank the referee for very constructive comments, which helped improve the manuscript tremendously. PC acknowledges support from the Department of Science and Technology via Swarana-Jayanti Fellowship award (file no. DST/SJF/PSA-01/2014-15). GAW acknowledges Discovery Grant support from the Natural Science and Engineering Research Council (NSERC) of Canada. AuD acknowledges support by NASA through Chandra Award numbers GO5-16005X, AR6-17002C, G06-17007B and proposal 18200020 issued by the Chandra X-ray Observatory Center which is operated by the Smithsonian Astrophysical Observatory for and behalf of NASA under contract NAS8- 03060. ADU gratefully acknowledges support from the *Fonds québécois de la recherche sur la nature et les technologies*, and DHC for NASA Chandra grants TM4-15001B and GO6-17007D. RHDT acknowledges support from NSF SI2 grant ACI-1339600 and NASA TCAN grant NNX14AB55G. The National Radio Astronomy Observatory is a facility of the National Science Foundation operated under cooperative agreement by Associated Universities, Inc.

REFERENCES

Abbott D. C., Bieging J. H., Churchwell E., 1985, in Hjellming R. M., Gibson D. M., eds, Astrophysics and Space Science Library, Vol. 116, Radio Stars: Observations of Nonthermal Emission from Early-Type Stars. Reidel Publ. Co., Dordrecht, p. 219
Alecian E. et al., 2008, A&A, 481, L99
Alecian E. et al., 2014, A&A, 567, A28
Babel J., Montmerle T., 1997, A&A, 323, 121
Bagnuolo W. G., Gies D. R., 1992, in McAlister H. A., Hartkopf W. I., eds, ASP Conf. Ser. Vol. 32, IAU Colloq. 135: Complementary Approaches to Double and Multiple Star Research. Astron. Soc. Pac., San Francisco, p. 140
Bailey J. D. et al., 2012, MNRAS, 423, 328
Benaglia P., Cappa C. E., Koribalski B. S., 2001, A&A, 372, 952
Bieging J. H., Abbott D. C., Churchwell E. B., 1989, ApJ, 340, 518
Blazère A., Neiner C., Tkachenko A., Bouret J.-C., Rivinius T., 2015, A&A, 582, A110
Blomme R., 2011, Bull. Soc. R. Sci. Liege, 80, 67
Bouret J.-C., Donati J.-F., Martins F., Escolano C., Marcolino W., Lanz T., Howarth I., 2008, MNRAS, 389, 75
Chandra P. et al., 2015, MNRAS, 452, 1245
Cohen D. H., Li Z., Gayley K. G., Owocki S. P., Sundqvist J. O., Petit V., Leutenegger M. A., 2014, MNRAS, 444, 3729
Drake S. A., Abbott D. C., Bastian T. S., Bieging J. H., Churchwell E., Dulk G., Linsky J. L., 1987, ApJ, 322, 902
Dufton P. L. et al., 2006, A&A, 457, 265
Eichler D., Usov V., 1993, ApJ, 402, 271
Grunhut J. H. et al., 2013, MNRAS, 428, 1686
Guarcello M. G., Caramazza M., Micela G., Sciortino S., Drake J. J., Prisinzano L., 2012, ApJ, 753, 117
Hummel C. A., Rivinius T., Nieva M.-F., Stahl O., van Belle G., Zavala R. T., 2013, A&A, 554, A52
Kharchenko N. V., Piskunov A. E., Röser S., Schilbach E., Scholz R.-D., 2004, Astron. Nachr., 325, 740
Krtička J., 2014, A&A, 564, A70
Lamers H. J. G. L. M., Leitherer C., 1993, ApJ, 412, 771
Leone F., 1991, A&A, 252, 198
Leto P., Trigilio C., Buemi C. S., Umana G., Leone F., 2006, A&A, 458, 831
Leto P., Trigilio C., Buemi C. S., Leone F., Umana G., 2012, MNRAS, 423, 1766
Linder N., Rauw G., Martins F., Sana H., De Becker M., Gosset E., 2008, A&A, 489, 713
Linsky J. L., Drake S. A., Bastian T. S., 1992, in Giampapa M. S., Bookbinder J. A., eds, ASP Conf. Ser. Vol. 26, Cool Stars, Stellar Systems, and the Sun. Astron. Soc. Pac., San Francisco, p. 325
Martayan C., Floquet M., Hubert A.-M., Fabregat J., Frémat Y., Baade D., Neiner C. 2007, in Bouvier J., Chalabaev A., Charobonnel C., eds, SF2A-2007: Proc. Annu. Meeting French Soc. Astron. Astrophys., Grenoble, France, p. 518
Morel T. et al., 2014, The Messenger, 157, 27
Nazé Y., Petit V., Rinbrand M., Cohen D., Owocki S., ud-Doula A., Wade G. A., 2014, ApJS, 215, 10
Olnon F. M., 1975, A&A, 39, 217
Owocki S. P., Rybicki G. B., 1984, ApJ, 284, 337
Owocki S., Townsend R., Ud-Doula A., 2008, Rev. Mex. Astron. Astrofis. Ser. Conf., 33, 80
Panagia N., Felli M., 1975, A&A, 39, 1
Petit V. et al., 2013, MNRAS, 429, 398
Pittard J. M., 2010, MNRAS, 403, 1633
Plaskett J. S., 1922, JRASC, 16, 284
Shore S. N., Brown D. N., Sonneborn G., Landstreet J. D., Bohlender D. A., 1990, ApJ, 348, 242
Shultz M., 2016, PhD thesis
Smith N., 2014, ARA&A, 52, 487
Stevens I. R., 1995, MNRAS, 277, 163

Trigilio C., Leto P., Umana G., Leone F., Buemi C. S., 2004, A&A, 418, 593
ud-Doula A., Owocki S. P., 2002, ApJ, 576, 413
ud-Doula A., Owocki S., Townsend R., Petit V., Cohen D., 2014, MNRAS, 441, 3600
Usov V. V., Melrose D. B., 1992, ApJ, 395, 575
van Loo S., Runacres M. C., Blomme R., 2005, A&A, 433, 313
van Loo S., Runacres M. C., Blomme R., 2006, A&A, 452, 1011
Vink J. S., de Koter A., Lamers H. J. G. L. M., 2000, A&A 362, 295
Wade G. A. et al., 2016, MNRAS, 456, 2
Weiler K. W., Panagia N., Montes M. J., Sramek R. A., 2002, ARA&A, 40, 387
Wheelwright H. E., Oudmaijer R. D., Schnerr R. S., 2009, A&A, 497, 487

This paper has been typeset from a TEX/LATEX file prepared by the author.